COMMUNICATION

ChemComm
www.rsc.org/chemcomm

Direct conversion of iron stearate into magnetic Fe and Fe_3C nanocrystals encapsulated in polyhedral graphite cages

Junfeng Geng, David A. Jefferson and Brian F. G. Johnson*

Department of Chemistry, Cambridge University, Lensfield Road, Cambridge, UK CB2 1EW. E-mail: bfgj1@cam.ac.uk; Fax: +44 (0)1223 336362; Tel: +44 (0)1223 336337

Received (in Cambridge, UK) 27th April 2004, Accepted 12th July 2004
First published as an Advance Article on the web 21st September 2004

We report a direct salt-conversion approach for large-scale synthesis of carbon-encapsulated magnetic Fe and Fe_3C nanoparticles.

Carbon-encapsulated magnetic metal nanoparticles, such as Fe, Ni and Co, have a core–shell structure.[1] The excellent stability towards environmental degradation makes these small particles ideal candidates in many applications such as magnetic data storage, magnetic toners in xerography and magnetic inks or ferrofluids,[2] as well as in bio-engineering applications such as drug delivery and magnetic resonance imaging.[3] These materials can be synthesised by the electrical arc-discharge technique[1–4] and pyrolysis of non-graphitising carbon materials,[5] however, the yield is low, which makes large-scale synthesis impractical. Recently, catalytically assisted chemical vapour deposition (CCVD) has been employed,[6] but some obstacles still limit the method for large-scale synthesis. These include problems caused either by the relatively low productivity, or the poor product quality, or difficulty in separating the product from the catalyst supporting material. In this paper we report a new method for bulk synthesis of the carbon-encapsulated magnetic iron nanoparticles. We find that the salt of iron stearate can be directly converted into Fe and Fe_3C nanocrystals encapsulated in polyhedral carbon cages on pyrolysis under appropriate conditions, and the direct salt-conversion phenomenon can be used as a single-step approach to make the material in large-scale.

The chemical process of the salt conversion may be understood from the following stoichiometric equation:

$$n(CH_3(CH_2)_{16}COO)_2^- \; Fe^{2+} \rightarrow n\mathrm{Fe} + (36n)\mathrm{C} + (4n)\mathrm{O} + (70n)\mathrm{H}$$

Formation of the metal nanoparticles by atomic aggregation was followed by a series of processes including segregation, diffusion and precipitation of the carbon on the particle surfaces, as well as nucleation and growth of the graphite cages through continuous carbon deposition. Some of the carbon may be lost as CO and CO_2. The H and O will be eventually released as H_2O. The conversion experiment was carried out at 900 °C under an argon atmosphere. To successfully realise the conversion process, we find that it is necessary to restrict the movement of the atomic carbon generated in the gas phase and thereby to let them be substantially maintained within the reactor. A comparative experiment shows that without this confinement, no carbon-encapsulated nanoparticles are produced under the same conditions.

Examination of the product by scanning electron microscopy (SEM) and transmission electron microscopy (TEM) indicates that the conversion has produced metal nanoparticles encapsulated in polyhedral graphite cages (Fig. 1 and 2). The nanoparticles are typically 20 to 200 nm in diameter, with 20 to 80 graphene layers on the wall. The metal cores are single crystals, as evidenced by the lack of grain boundaries in the HRTEM images. The carbon shells are also highly crystalline. Evidence of 3-dimensional crystallinity in the graphitic structure comes from the presence of (10*l*) fringes observed crossing the 3.4 Å layer fringes. The encapsulation occurs independently of the particle size. No naked Fe nanoparticles have been observed under intensive microscope observations. This is in contrast to the arc-discharge technique where the naked metal particles are the main side-product. Thus, in regard to the stoichiometric conversion of Fe, our yield approximates to 100%.

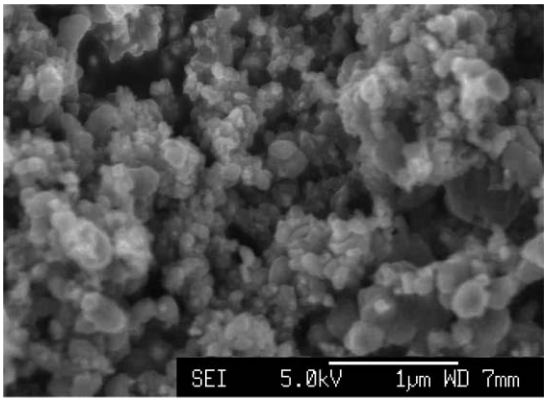

Fig. 1 SEM image of the as-converted product shows the nanoparticles and their size distribution. The product was prepared by placing *ca.* 3.0 g iron stearate powder (Strem Chemicals Ltd., dark brown pills, needs to be ground before use) in a quartz reactor that was then placed at the centre of a tube-shaped furnace. A flow of argon (1.5–2.0 l min^{-1}) was employed to get rid of gases produced during the thermal decomposition. The reaction temperature was 900 °C, reaction time was 10 min.

X-ray diffraction tests on the as-prepared products confirm that the encapsulated species are either single-phase metallic Fe or Fe_3C single crystals (Fig. 3).† The narrow peak at $2\theta = 26.3°$ results from well-crystallised graphite (002) fringes with a *d*-spacing of 3.39 Å. A laser Raman test shows the normal D and G peaks of graphitic structure at 1353 cm^{-1} and 1582 cm^{-1}, respectively, with the intensity of G > D. At present it is still not possible to determine the ratio between Fe and Fe_3C.[7] However, it is reasonable to believe, based on our electron microscopic observations and the X-ray result, that neither Fe nor Fe_3C dominates in the product. To investigate the magnetic properties, the magnetization of the encapsulated particles *versus* the applied field at room temperature (300 K) was measured with a maximum applied field of 50 kOe. The observed *M*–*H* loop (Fig. 4) indicates the intrinsic magnetic properties of the nanoparticles. The saturation magnetization (M_s), remanent magnetization (M_r) and coercive field (H_c) are measured as 58.8 emu g^{-1}, 5.0 emu g^{-1} and 240 Oe, respectively.‡

The stability of the encapsulated products was tested by heating the sample in air to 400 °C, followed by a slow cooling procedure to room temperature over 12 h. The heated sample shows no change in either sample weight or colour, suggesting good thermal stability together with strong resistance to oxidation. This excellent property obviously arises from the completely closed carbon structures. The high thermal stability is also confirmed by the observation that no degradation occurs at room temperature for over one year, and no structural change in the heated sample can be seen in TEM investigations.

In contrast to the electrical arc-discharge technique, this direct salt-conversion route gives far higher yields at a much lower temperature. Similarly, in comparison with the chemical vapour deposition (CVD) method, our new technique does not require a

DOI: 10.1039/b406227b

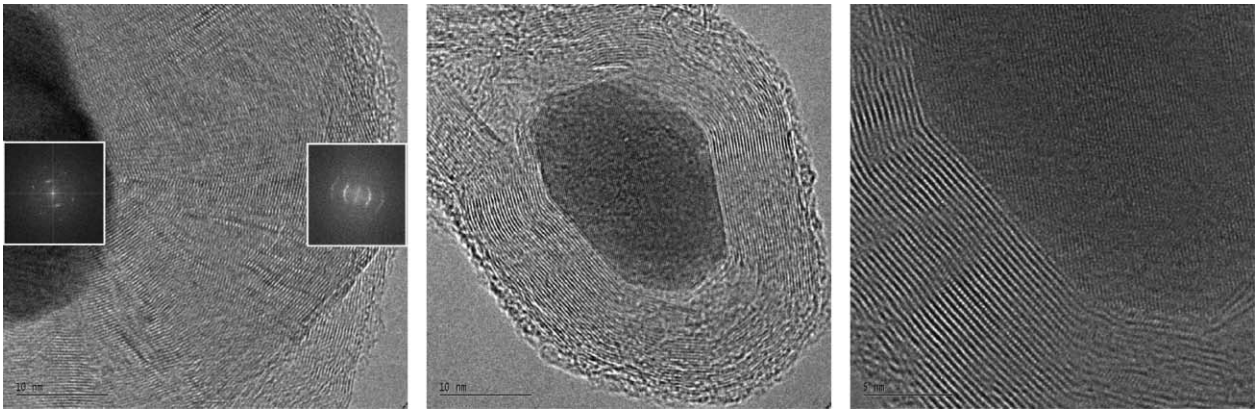

Fig. 2 HRTEM images of the carbon-encapsulated iron nanoparticles. From left to right, (a), (b) and (c), respectively. (a) The power spectrum of the central particle shows maxima corresponding to graphite (002), (004) and (10*l*) fringes. The crystal lattice gives a spacing of 2.03 Å, corresponding to Fe (110) fringes [d = 2.035 Å]. (b) HRTEM image of another encapsulated particle. (c) A higher magnification image of the same particle shown in (b), shows the well crystalline graphite at atomic resolution, and the atomically smooth interface between graphite and the encapsulated nanocrystal. Using the graphite fringes as reference, the crystal lattice spacing is measured as 2.22 Å, corresponding to Fe_3C (201) [d = 2.219 Å].

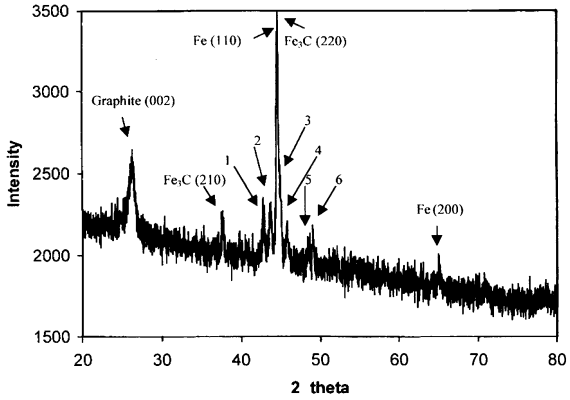

Fig. 3 The X-ray diffraction pattern of the as-converted iron product. Apart from the peaks shown on the spectrum, the peaks labelled 1 to 6 have been indexed as follows: 1: Fe_3C (211); 2: Fe_3C (102); 3: Fe_3C (031); 4: Fe_3C (112); 5: Fe_3C (131); 6: Fe_3C (221).

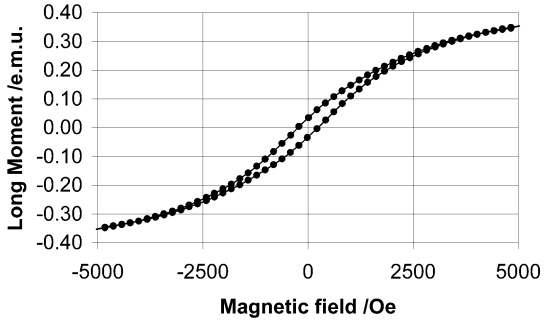

Fig. 4 Magnetic measurement (hysteresis loop) for the as-converted sample which is the same as that employed in the X-ray test. The sample weight used in this measurement is 6.8 mg.

separate carbon feedstock or catalyst support. These advantages not only simplify the synthetic process but also avoid the after-growth separation of product from catalyst support. As far as we can judge this is the first example of such an effective, simple and single-step method. In addition, we believe that the direct salt-conversion phenomenon is neither limited to iron, nor the stearate. In general, this new method opens up a way to the exploration of the bulk synthesis of carbon-encapsulated metal nanoparticles from conversion of organic or inorganic salts that have sufficiently large number of carbon atoms within their molecular structures.

We are grateful for financial support from Thomas Swan & Co. Ltd., UK. We thank help given by Dr. Bill Jones (Department of Chemistry, Cambridge University) and Mr. Douglas Astill (IRC research centre, Cambridge University).

Notes and references

† The mechanism for formation of the Fe_3C nanocryatals remains unclear and thus open to question. We believe that they may arise from the transformation of FeO (produced by reaction of Fe with O, due to some residence time of O in the reactor caused by sample confinement) in the presence of atomic carbon and hydrogen in the gas phase. This possible mechanism is similar to the case studied by Emmenegger *et al.*[8] using Fe nanoparticles as catalyst for growing carbon nanotubes where formation of the Fe_3C was measured by *in situ* X-ray experiments.

‡ The saturation magnetisation is 27.1% of that of the bulk polycrystalline iron (300 K, 217.2 emu g^{-1})[9] suggesting magnetic character close to superparamagnetism.

1 S. Subramoney, *Adv. Mater.*, 1998, **10**, 1157; P. J. Harris, in *Carbon Nanotubes and Related Structures — new materials for the twenty-first century*, Cambridge University Press, Cambridge, 1999, ch. 5.
2 R. S. Ruoff, D. C. Lorents, B. Chan, R. Malhotra and S. Subramoney, *Science*, 1993, **259**, 346; V. P. Dravid, J. J. Host, M. H. Teng, B. Elliot, J. Hwang, D. L. Johnson, T. O. Mason and J. R. Weertman, *Nature*, 1995, **374**, 602; T. Hayashi, S. Hirono, M. Tomita and S. Umemura, *Nature*, 1996, **381**, 772.
3 A. A. Bogdanov, C. Martin, R. Weissleder and T. J. Brady, *Biochim. Biophys. Acta*, 1994, **1193**, 212; S. G. Fitzpatrick-McElligott, J. G. Lavin, G. F. Rivard and S. Subramoney, *US Patent 5,466,587*, 1995.
4 J. H. T. Scott and S. A. Majetich, *Phys. Rev. B*, 1995, **52**, 12564; S. Seraphin, D. Zhou and J. Jiao, *J. Appl. Phys.*, 1996, **80**, 2097.
5 P. J. F. Harris and S. C. Tsang, *Chem. Phys. Lett.*, 1998, **293**, 53.
6 B. H. Liu, J. Ding, Z. Y. Zhong, Z. L. Dong, T. White and J. Y. Lin, *Chem. Phys. Lett.*, 2002, **358**, 96; E. Flahaut, F. Agnoli, J. Sloan, C. O'Connor and M. L. H. Green, *Chem. Mater.*, 2002, **14**, 2553; Z. Zhong, H. Chen, S. Tang, J. Ding, J. Lin and K. L. Tan, *Chem. Phys. Lett.*, 2000, **330**, 41.
7 X. Sun, A. Gutierrez, M. J. Yacaman, X. Dong and S. Jin, *Mater. Sci. Eng., A*, 2000, **286**, 157.
8 C. Emmenegger, J.-M. Bonard, P. Mauron, P. Sudan, A. Lepora, B. Grobety, A. Züttel and L. Schlapbch, *Carbon*, 2003, **41**, 539.
9 C. D. Graham, Jr, *J. Appl. Phys.*, 1996, **53**, 2032.